

## Weak ferromagnetism and canting in $\text{BiPbSr}_2\text{MnO}_6$ and $\text{BiPbCa}_2\text{MnO}_6$

W. R. McKinnon and E. Tselepis

*National Research Council of Canada, Ottawa, Ontario, Canada K1A 0R9*

J. M. Tarascon, P. F. Miceli, K. Remschnig, and G. W. Hull

*Bell Communications Research, Red Bank, New Jersey 07701*

D. A. Neumann and J. J. Rhyne

*National Institute for Standards and Technology, Gaithersburg, Maryland 20899*

(Received 26 September 1990; revised manuscript received 26 November 1990)

The magnetic behavior of single crystals and powders of  $\text{BiPbSr}_2\text{MnO}_6$  and  $\text{BiPbCa}_2\text{MnO}_6$  has been measured between 300 and 4 K. These analogues of the high-temperature superconducting bismuth cuprates have no structural modulation, and consequently do not have the sharp peak in magnetization found in modulated  $\text{Bi}_2\text{Sr}_2\text{MnO}_{6+\delta}$ . Instead, their magnetic behavior is consistent with antiferromagnetism (below transition temperatures near 150 K in crystals and 200 K in powders) with the spins mainly oriented normal to the  $\text{MnO}_2$  planes, as confirmed by neutron diffraction. They also show weak ferromagnetism, with a remanent moment in the  $\text{MnO}_2$  planes; this is interpreted as small canting (less than  $0.1^\circ$ ) of the spins toward the  $\text{MnO}_2$  planes.

### I. INTRODUCTION

Layered bismuth cuprates in the family  $\text{Bi}_2\text{Sr}_2\text{Ca}_{n-1}\text{Cu}_n\text{O}_{6+2n+\delta}$  are high-temperature superconductors.<sup>1,2</sup> Related compounds with Cu replaced by other transition metals are not,<sup>3</sup> but studies of their structure and magnetic properties may help understand the superconductivity of the cuprates. For example, the solution of the structure<sup>4</sup> in  $\text{Bi}_2\text{Sr}_3\text{Fe}_2\text{O}_{9.2}$  showed that extra oxygen in the Bi-O layers is responsible for the strong structural modulation also seen in the cuprates.<sup>5</sup> The superconductivity in the cuprates undoubtedly originates in the  $\text{CuO}_2$  layers, whereas the modulation is associated with another part of the structure; consequently, the only connection between the modulation and superconductivity is that the extra oxygen in the Bi-O layers provides a mechanism of doping the  $\text{CuO}_2$  layers. This conclusion was recently strengthened by the demonstration that superconductivity persists in  $\text{Bi}_{2-x}\text{Pb}_x\text{Sr}_{2-y}\text{La}_y\text{CuO}_6$  when  $x$  and  $y$  are adjusted to eliminate the distortion.<sup>6</sup>

The modulation has a more direct effect on magnetism in these layered materials. In the bismuth manganate  $\text{Bi}_2\text{Sr}_2\text{MnO}_{6+\delta}$ , the magnetic susceptibility has a sharp peak at 120 K accompanying the onset of antiferromagnetic ordering; at lower temperatures, the compound has a field-induced transition and irreversible magnetic behavior.<sup>7</sup> The modulation produces different types of Mn sites in the  $\text{MnO}_2$  layers, and it was proposed that the moments of the Mn ions on adjacent sites do not cancel in the ordered state. A simple mean-field model of ferromagnetic layers explains the sharp peak and the field-induced transition. Consistent with this explanation, the sharp anomaly disappears in powders of  $\text{BiPbSr}_2\text{MnO}_6$ , in which there is no modulation and all Mn sites are crystallographically equivalent.<sup>8</sup>

This paper extends our work on the nonmodulated analogues of the bismuth cuprates, with experimental results of the magnetism in single crystals and powders of  $\text{BiPbSr}_2\text{MnO}_6$  and  $\text{BiPbCa}_2\text{MnO}_6$ .

### II. METHODS

Single crystals of  $\text{BiPbSr}_2\text{MnO}_6$  and  $\text{BiPbCa}_2\text{MnO}_6$  were made from stoichiometric amounts of  $\text{SrCO}_3$  or  $\text{CaCO}_3$ ,  $\text{MnO}_2$ , and 50% excess of  $\text{Bi}_2\text{O}_3$  and  $\text{PbO}$ . The excess material serves as the flux. About 20 g of the starting materials were ground and placed in an alumina crucible. The crucible was heated in nitrogen to a temperature  $T_1$  in 8 h, held for 1.75 h, and cooled to 800°C in 50 h. The temperature  $T_1$  was 1300°C for Sr and 1200°C for Ca. The furnace was then switched off, and the crucible was removed when the furnace had cooled. Platelike crystals as large as 5–6 mm on an edge and 0.1 mm thick grew in cavities in the melt. Powder x-ray diffraction confirmed that, as usual, the  $c$  axis is normal to the plane of the platelets. The structure of  $\text{BiPbSr}_2\text{MnO}_6$  determined from a crystal from one of these batches has been reported elsewhere.<sup>8</sup>

Powders were made from stoichiometric amounts of the above materials, reacted at 960°C in nitrogen for 48 h, and furnace cooled. The powders of  $\text{BiPbSr}_2\text{MnO}_6$  were pure, but those of  $\text{BiPbCa}_2\text{MnO}_6$  were contaminated by  $\text{Ca}_2\text{MnO}_4$  and other phases. Some of our magnetic results on powders of the Sr compound have been reported elsewhere as part of a study of the effects of partially replacing Mn by Zn and Ni.<sup>9</sup> We could not measure magnetization in powders of the Ca compound because of the strong ferromagnetism of the impurity phases, but we were able to see the magnetic ordering with neutron diffraction.

Magnetization was measured with a Quantum Design or a S.H.E. SQUID magnetometer. Crystals were aligned by eye, glued to a thread, and hung in the detection coils. Because of the weak ferromagnetism discussed below, crystals can develop a moment that is not parallel to the applied field. At fields much above 5 kG, the resulting torque can twist the crystal despite the glass weight hanging on the end of the thread. On the other hand, because the crystals we studied are small (3 mg at most), we could not get good results at lower fields, so we did most measurements of crystals with 5 kG. Magnetization of powder could be measured at lower fields. We studied the angular dependence of magnetization of one crystal in the S.H.E. magnetometer with a transverse detector coil. In this measurement, we cooled a crystal in zero field and rotated it about  $c$  while measuring  $M_r$  in the  $ab$  plane. Resistance of pellets of  $\text{BiPbSr}_2\text{MnO}_{6+\delta}$  was measured with a four-probe technique.

One rectangular crystal of  $\text{BiPbSr}_2\text{MnO}_6$  was aligned with single-crystal x-ray diffraction. In this crystal, the  $c$  axis was normal to the plane of the platelet, and the crystallographic  $a$  and  $b$  axes were parallel to the edges. We assumed that in other rectangular crystals  $a$  and  $b$  were also parallel to the edges of the rectangle.

Neutron diffraction was performed at the Neutron Beam Split-Core Reactor at the National Institute of Standards and Technology, with the same spectrometer and procedure described in Ref. 7. Powder samples of  $\text{BiPbSr}_2\text{MnO}_6$  and  $\text{BiPbCa}_2\text{MnO}_6$  as prepared under nitrogen, and of  $\text{BiPbSr}_2\text{MnO}_{6+\delta}$  annealed in oxygen, were measured both above the ordering temperatures and at 9 K. The data were corrected for thermal expansion and subtracted to obtain the magnetic Bragg intensity.

### III. MAGNETIZATION MEASUREMENTS

The results for the Ca compound are easier to understand, so we describe them first. Figure 1(a) shows the magnetization  $M$  versus temperature  $T$  for field  $H$  parallel and perpendicular to  $c$ . These data were obtained for two large platelets of irregular shape, so the orientations in the  $ab$  plane are not known. The results were measured as the sample was cooled in the field, but the results for warming in a field are similar, provided the sample has been previously cooled in the same field. For samples cooled in fields near zero, however, the results below 160 K for  $H$  in the  $ab$  plane depend sensitively on the field during cooling. The inset in Fig. 1(a) shows on an expanded scale the broad maximum in  $M$  above  $T_N$ . This maximum, also seen in other layered manganates,<sup>10,11</sup> makes it impossible to extract the Mn moment from a Curie-Weiss plot of our data, which only extend to 300°C.

For  $H$  along  $c$ ,  $M$  is just as expected for an antiferromagnet with the spins parallel and antiparallel to  $c$ ; the susceptibility drops below the transition temperature,  $T_N = 160$  K. But for a simple antiferromagnet, the susceptibility perpendicular to the spins (in the  $ab$  plane) should be constant below  $T_N$ . As the figure shows, it is not; it increases below  $T_N$  as  $T$  decreases.

The extra  $M$  below  $T_N$  is a remanent magnetization; it

remains if the field is turned off. Moreover, it varies with the relative orientation of the crystal and the field. Figure 1(b) shows the remanent magnetization  $M_r$  versus  $T$  as a single crystal is warmed in zero field after it had been cooled in a field  $H$  in one of three orientations in the  $ab$  plane. The maximum signal is for a field at 45° to  $a$  and  $b$ . We label this direction  $[110]$ . The value of  $M_r$  at 10 K is  $25 \times 10^{-3}$  emu/g corresponding to a moment of  $0.0029\mu_B$  per Mn. The minimum (nearly zero) is 90° to  $[110]$ ; we label this direction  $[\bar{1}10]$ . Note that the signs in these labels are arbitrary, because in the crystal structure of  $\text{BiPbSr}_2\text{MnO}_6$  determined in Ref. 8, these two directions are equivalent. Along both  $a$  and  $b$ , the signal is about  $1/\sqrt{2}$  times the maximum signal. [Only the data along  $a$  are shown in Fig. 1(b).]

The relative size of  $M_r$  along the various directions in the  $ab$  plane is consistent with the notion that  $M_r$  points along  $[110]$  no matter what direction the field was pointing during cooling. We verified this by cooling a crystal in the remanent field of the magnet (a few gauss) in a squid with a transverse coil. As the crystal rotated about  $c$ , with the squid detector coils measuring  $M$  in the  $ab$

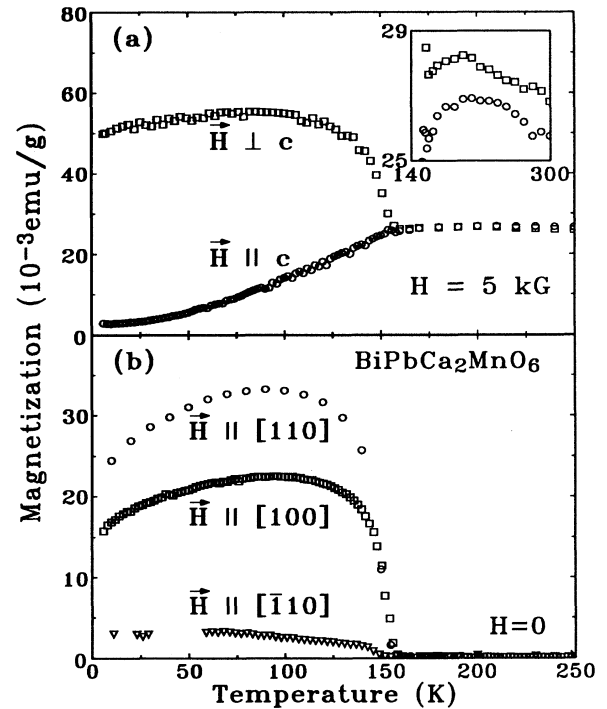


FIG. 1. (a) Magnetization  $M$  vs temperature  $T$  for two crystals (total mass 4.1 mg) of  $\text{BiPbCa}_2\text{MnO}_6$  cooling in a field  $H$  of 5 kG, oriented parallel and perpendicular to  $c$ . The inset shows an expanded vertical scale for the region above the transition. In the inset, the data for  $H$  parallel to  $c$  (squares) have been shifted up for clarity. (b) Magnetization  $M$  vs temperature  $T$  for a 1-mg crystal of  $\text{BiPbCa}_2\text{MnO}_6$ , measured on warming in zero field after the sample had cooled in 500 G, for three directions in the  $ab$  plane. In this rectangular crystal, the  $[100]$  and  $[010]$  directions were assumed to lie along the edges of the rectangle.

plane, the signal varied sinusoidally, with its maxima and minima in directions  $45^\circ$  to  $a$  and  $b$ . Thus a crystal behaves like a classical antiferromagnet for  $H$  along  $c$  or along  $[\bar{1}10]$ . In the third direction, along  $[110]$ , it looks like an antiferromagnet with a superimposed ferromagnetic component.

For  $H$  in the  $ab$  plane, the Sr compound  $\text{BiPbSr}_2\text{MnO}_6$  behaves just like the Ca compound. Figure 2(a) shows  $M(T)$  for  $H$  perpendicular to  $c$  along the two directions  $[110]$  and  $[\bar{1}10]$ . This rectangular crystal was subsequently oriented by x-ray diffraction, confirming that  $a$  and  $b$  were along the edges of the crystal. (In the Ca crystal discussed above, it was assumed that  $a$  and  $b$  also lay along the edges.) For the  $[110]$  direction, the remanent moment per Mn ion is  $40 \times 10^{-3}$  emu/g at 10 K, corresponding to  $0.0053\mu_B$  per Mn.

For  $H$  parallel to  $c$ ,  $\text{BiPbSr}_2\text{MnO}_6$  is more complicated than  $\text{BiPbCa}_2\text{MnO}_6$ . Figure 2(b) shows  $M(T)$  for  $H$  parallel to  $c$  as the crystal is warmed in a field, either after cooling in the same field or after cooling in zero field. The magnetization depends on the previous history, somewhat analogous to the behavior in  $\text{Bi}_2\text{Sr}_2\text{MnO}_{6+\delta}$  below 40 K. When the sample is cooled in a field, the

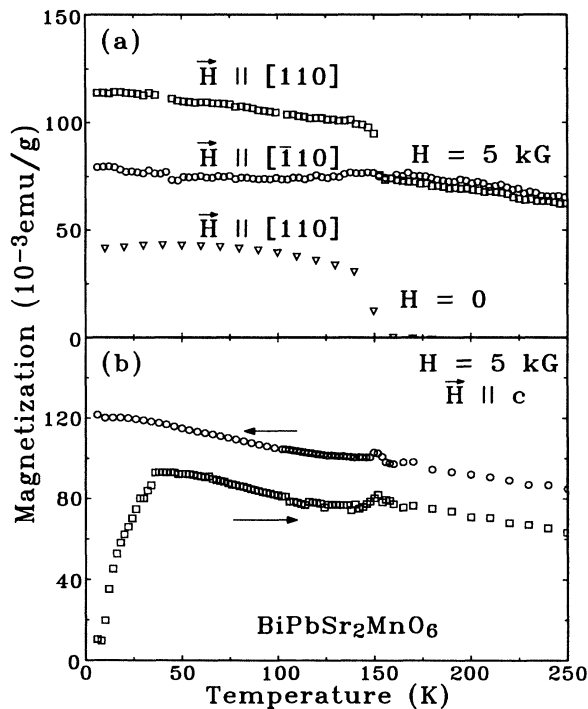


FIG. 2. (a) Magnetization  $M$  vs temperature  $T$  for a 0.4-mg crystal of  $\text{BiPbSr}_2\text{MnO}_6$ . This crystal was oriented by x-ray diffraction. The two upper curves are for cooling in 5 kG with the field in two directions at  $45^\circ$  to  $a$  and  $b$ . The lower curve is for warming in zero field following cooling in 5 kG. (b) Magnetization  $M$  vs temperature  $T$  for a 2.6-mg crystal of  $\text{BiPbSr}_2\text{MnO}_6$  for cooling and warming in a field of 5 kG along the  $c$  axis. The data for cooling (circles) have been shifted upward for clarity.

magnetization remains constant below  $T_N$ . If the sample is cooled in zero field and then warmed in a field, the magnetization increases to meet the cooling curve at about 40 K. [Note that the two curves in Fig. 2(b) are offset for clarity.] The magnetization shows a small peak at  $T_c$ , much smaller than observed in  $\text{Bi}_2\text{Sr}_2\text{MnO}_{6+\delta}$ , but in contrast to  $\text{BiPbCa}_2\text{MnO}_6$ , which shows no such peak.

In powders of  $\text{BiPbSr}_2\text{MnO}_6$ , the transition as measured by the peak in  $M$  occurs at a higher temperature, 195 instead of 150 K. Figure 3 shows  $M(T)$  for a powder of  $\text{BiPbSr}_2\text{MnO}_6$  cooling in a magnetic field [the curve labeled  $\text{N}_2(1)$ ]. The ferromagnetic component appears at about 190 K. Similarly, the transition temperature of  $\text{BiPbCa}_2\text{MnO}_{6+\delta}$  powder is shifted to 180 K, as was found by neutron diffraction (see below). The difference in the synthesis temperatures of the crystals and powders may lead to small differences in stoichiometry, perhaps explaining the changes in the magnetic ordering temperature.

When  $\text{BiPbSr}_2\text{MnO}_6$  is heated in oxygen, it takes up oxygen and the structural modulation reappears.<sup>8</sup> We attempted to study the magnetism in oxygenated crystals, but found that the uptake of oxygen takes many weeks and damages the crystals. In powders, however, oxygen is absorbed much faster, according to our thermogravimetric analysis (TGA) measurements. Pure single-phase powders (as determined by x rays) could be obtained by heating powder in a TGA apparatus at  $5^\circ/\text{min}$  to  $600^\circ\text{C}$ . Figure 3 compares  $M(T)$  for a powder of  $\text{BiPbSr}_2\text{MnO}_{6+\delta}$  as grown in nitrogen, after annealing in oxygen, and after reannealing in nitrogen. The magnetic transition shifts from 200 to 90 K when the sample is annealed in oxygen. The changes in  $M(T)$  below 90 K for the oxygen-annealed sample are due to a remanent magnetization, as we confirmed by cooling a sample in a field and warming it in zero field. The reversal in sign of  $M(T)$  may be due to a variation of the spin canting with temperature, as discussed below. When the sample was

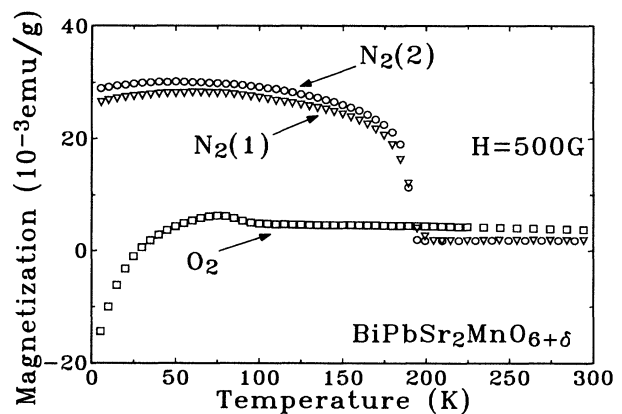


FIG. 3. Magnetization  $M$  vs temperature  $T$  for powder of  $\text{Bi}_2\text{Sr}_2\text{MnO}_{6+\delta}$  as prepared in nitrogen [ $\text{N}_2(1)$ ], after annealing in oxygen ( $\text{O}_2$ ), and after reannealing in nitrogen [ $\text{N}_2(2)$ ], for cooling in a field of 500 G.

reannealed in nitrogen, the transition temperature and amplitude of the magnetization were restored, indicating that there was no decomposition of the material during either annealing steps. The resistance of a pellet of  $\text{BiPbSr}_2\text{MnO}_{6+\delta}$  dropped by a factor of about 1000 when the pellet was annealed in oxygen, and increased again when it was reannealed in nitrogen.

#### IV. NEUTRON-DIFFRACTION RESULTS

Figure 4 shows the magnetic powder neutron diffraction for powders of  $\text{BiPbSr}_2\text{MnO}_{6+\delta}$  as prepared in nitrogen [Fig. 4(a)] and annealed in oxygen for 1 h at  $600^\circ\text{C}$  [Fig. 4(b)]. As Table I indicates, the relative intensities of the magnetic reflections do not change with annealing, and are consistent with a model where the spins are antiferromagnetically aligned (nearest-neighbor spins oppositely directed), with the spins directed perpendicular to the  $\text{MnO}_2$  planes. This is the same spin

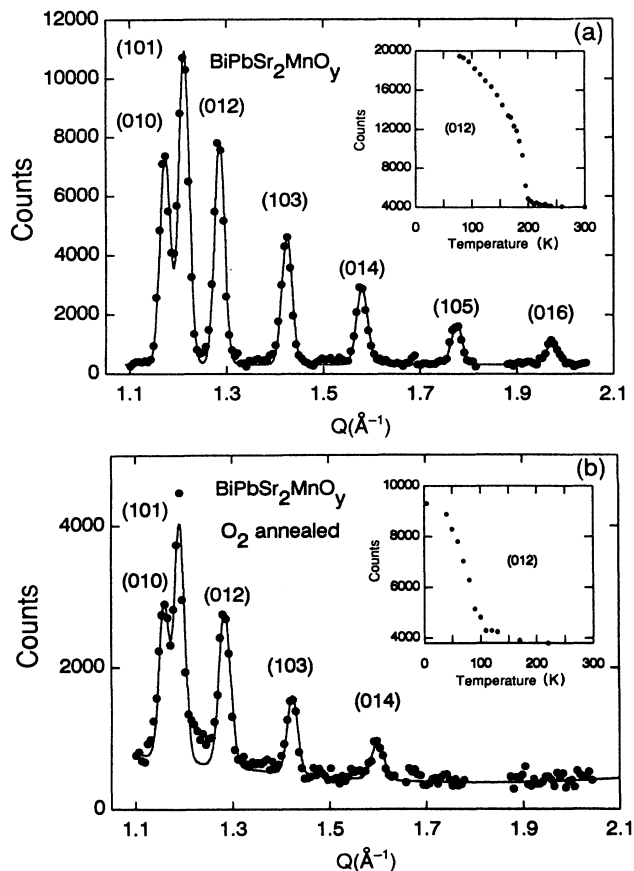


FIG. 4. Magnetic neutron powder diffraction for  $\text{Bi}_2\text{Sr}_2\text{MnO}_{6+\delta}$  (a) as prepared in nitrogen and (b) after annealing in oxygen, obtained by subtracting data taken above the transition from data taken at 9 K. The solid curves are from least-squares fits of the peaks to a Gaussian line shape and were used in determining the integrated intensity. The inset shows the temperature dependence of the (012) reflection, taken on cooling in zero field.

TABLE I. Relative intensities obtained from Fig. 7 for  $\text{BiPbSr}_2\text{MnO}_{6+\delta}$  compared to the calculated intensities assuming moments directed along the  $c$  axis and the antiferromagnetic-ordering wave vector along the [010] direction. (The calculated intensities are the same for ordering along [100], but the first two indices in the labeling of the peaks are interchanged.) The (101) intensities are normalized to 100. The statistical uncertainty on each of the measured relative intensities is  $\pm 2$  for the sample prepared in  $\text{N}_2$ , and  $\pm 4$  for the sample annealed in  $\text{O}_2$ .

Reflection	Relative Intensities		Calculated
	Prepared in $\text{N}_2$	Annealed in $\text{O}_2$	
(010)	66	66	55
(101)	100	100	100
(012)	68	75	73
(103)	40	33	47
(014)	26	19	28
(105)	13		16
(016)	8		9

configuration as observed in powder diffraction of  $\text{Bi}_2\text{Sr}_2\text{MnO}_{6+\delta}$  in Ref. 7. Both here and in our work on  $\text{Bi}_2\text{Sr}_2\text{MnO}_{6+\delta}$ , the small ferromagnetic moments seen in the magnetic measurements cannot be observed in the powder diffraction data.

The peaks in Fig. 4 appear at values of  $Q$  corresponding roughly to the average of  $a$  and  $b$ , rather than to either  $a$  or  $b$  alone. This indicates domains, with antiferromagnetic wave vectors along  $a$  in some domains and along  $b$  in others. This point will be studied in higher-resolution experiments on a single crystal.

The insets in Fig. 4 show the temperature dependence of the magnetic scattering. The oxygen annealing lowers the transition temperature by 100 K. The onset of the or-

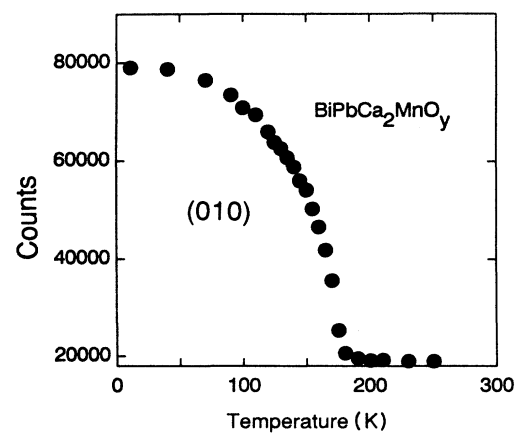


FIG. 5. The intensity of the (012) magnetic reflection for a powder of  $\text{Bi}_2\text{Ca}_2\text{MnO}_6$  prepared in nitrogen, obtained as in Fig. 4 by subtracting data at 9 K and above the transition temperature.

dering in the oxygen-annealed sample occurs at the same temperature as the small increase in magnetization below 100 K in Fig. 3.

We also studied a powder sample of  $\text{BiPbCa}_2\text{MnO}_6$  prepared in nitrogen. The temperature dependence of the (010) reflection, shown in Fig. 5, shows that the transition temperature is nearly the same as for the Sr compound prepared in nitrogen. The Ca sample contained impurity phases and we could not extract accurate peak intensities to include in Table I. But given the similarities in structure, transition temperature, and magnetic behavior of the Sr and Ca compounds, it is likely that both have the same arrangement of spins.

## V. DISCUSSION

The interpretation of the ordering in  $\text{BiPbCa}_2\text{MnO}_6$  is straightforward. The drop in magnetization for  $H$  along  $c$  below  $T_c$  clearly suggests an antiferromagnet with the spins aligned parallel or antiparallel to  $c$ , or nearly so. The magnetization in one direction normal to  $c$  is constant below  $T_N$ , consistent with this interpretation. Powder neutron diffraction confirms this spin arrangement in the Sr compound  $\text{BiPbSr}_2\text{MnO}_6$ .

The remanent moment along the other direction normal to  $c$  suggests a canting of spins along one of the  $[110]$  directions, as sketched in Fig. 6. (The figure shows the spins canted along  $[110]$ , but we cannot rule out that they are canted along  $[\bar{1}10]$ .) Consistent with this interpretation, the magnetization along  $a$  or  $b$  is  $1/\sqrt{2}$  times this maximum value. Thus the spins cant along one of the directions defined by Mn—O—Mn bonds. If the Mn is all  $\text{Mn}^{3+}$  of spin 2, and if the canting is the same in every  $\text{MnO}_2$  layer, then the canting angle is  $0.042^\circ$  in  $\text{BiPbCa}_2\text{MnO}_6$ . In the  $ab$  plane,  $\text{BiPbSr}_2\text{MnO}_6$  has the same behavior, with one  $[110]$  direction showing a remanent moment and the other not; the remanent moment implies a canting angle of  $0.076$  for  $\text{Mn}^{3+}$ . For the structure to have a net moment, spins in adjacent layers must cant in the same direction.

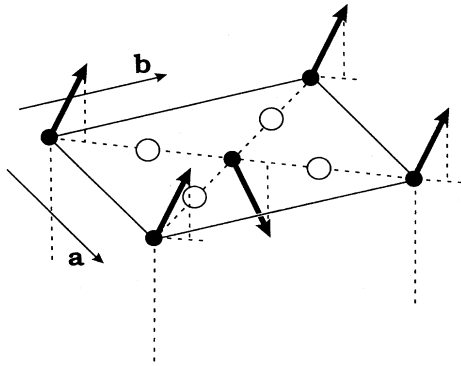


FIG. 6. Perspective view of the proposed ordering in  $\text{BiPbCa}_2\text{MnO}_6$  and  $\text{BiPbSr}_2\text{MnO}_6$ . The spins are canted along the left-right diagonal in the unit cell. The degree of canting has been exaggerated.

In the crystallographic structure found in Ref. 8 for  $\text{BiPbSr}_2\text{MnO}_6$ , there are no symmetry elements along or perpendicular to the Mn—O—Mn directions or midway between them, so the vector coupling constant of an antiferromagnetic exchange is not constrained by Moriya's rules.<sup>12</sup> There is nothing in the structure to explain why the spins should cant along one  $[110]$  direction (along Mn—O—Mn bonds) but not the other (which we have denoted  $[\bar{1}10]$ ) but the crystals clearly behave differently when the field is rotated by  $90^\circ$  in the  $ab$  plane, so something must distinguish these  $[110]$  directions.

As discussed in Ref. 8, the crystal structure determined there does not account for weak superlattice spots seen in electron-diffraction microscopy. These spots may indicate a superlattice that might break the symmetry between  $[110]$  and  $[\bar{1}10]$  and explain the difference in magnetism along these two directions. Alternatively, perhaps a further distortion develops below room temperature, although if so it must be small, because no distortion was found by neutron diffraction on powders.

The broad peak in  $M$  above the transition [shown in the inset to Fig. 1(a)] is probably caused by two-dimensional fluctuations in the  $\text{MnO}_2$  plane. Similar peaks in other layered manganates have been attributed to these two-dimensional effects.<sup>10,11</sup> These peaks were not observed in the modulated structures  $\text{Bi}_2\text{Sr}_2\text{MnO}_{6+\delta}$  or  $\text{Bi}_2\text{Ca}_2\text{MnO}_{6+\delta}$ .<sup>7</sup> It may be that the ferromagnetism in the individual layers in these modulated structures suppresses this peak.

Given the similarity of  $\text{BiPbCa}_2\text{MnO}_6$  and  $\text{BiPbSr}_2\text{MnO}_6$  in the  $ab$  plane, the behavior of  $\text{BiPbSr}_2\text{MnO}_6$  for fields along  $c$  is puzzling. The history dependence suggests some sort of spin-glass or domain behavior. In  $\text{Bi}_2\text{Sr}_2\text{MnO}_{6+\delta}$ , this dependence was not understood quantitatively, but it was suggested to be due to some remnant domains of the ferrimagnetic phase to which the bulk of the sample transforms at high field. In  $\text{BiPbSr}_2\text{MnO}_6$  we found no high-field phase to invoke as an explanation, although the powder neutron data suggests that there may be domains. Neutron diffraction of single crystals may help solve this puzzle.

The magnetic ordering shown by powders of  $\text{BiPbSr}_2\text{MnO}_{6+\delta}$  annealed in oxygen will be difficult to unravel without single crystals. Neutron diffraction confirms that the phase transition occurs at 100 K, where the magnetization starts to rise suddenly as the temperature drops. The subsequent drop and change in sign of  $M$  at lower temperatures suggest that the moments may vary in size or orientation with temperature. Because we have only powder information, we do not know whether this remanent moment is due to canting, as in  $\text{BiPbSr}_2\text{MnO}_6$  prepared in oxygen, or to moments of different sizes on different sites, as in  $\text{Bi}_2\text{Sr}_2\text{MnO}_{6+\delta}$ . The magnetization of oxygen-annealed  $\text{BiPbSr}_2\text{MnO}_{6+\delta}$  does not have a sharp peak like that seen in  $\text{Bi}_2\text{Sr}_2\text{MnO}_{6+\delta}$ , even though both compounds have a structural modulation. Perhaps differences in the interaction between layers causes  $\text{BiPbSr}_2\text{MnO}_{6+\delta}$  to form the ferrimagnetic phase, where the net moments of different layers add (as was suggested in Ref. 7 for  $\text{Bi}_2\text{Ca}_2\text{MnO}_{6+\delta}$ ); in

$\text{Bi}_2\text{Sr}_2\text{MnO}_{6+\delta}$ , the net moments of different layers cancel at low fields to form a true antiferromagnetic phase.

The transition temperatures of  $\text{Bi}_2\text{Sr}_2\text{MnO}_{6+\delta}$  and of oxygen-annealed  $\text{BiPbSr}_2\text{MnO}_{6+\delta}$  are both lower than that for as-prepared  $\text{BiPbSr}_2\text{MnO}_6$ . This correlates, perhaps coincidentally, with the presence of a single Mn valence ( $\text{Mn}^{3+}$ ) in as-prepared  $\text{BiPbSr}_2\text{MnO}_6$  compared to two Mn valences in  $\text{Bi}_2\text{Sr}_2\text{MnO}_{6+\delta}$  and oxygen-annealed  $\text{BiPbSr}_2\text{MnO}_{6+\delta}$ . The resistance of the mixed-valence compounds is also lower than that of as-prepared  $\text{BiPbSr}_2\text{MnO}_6$ , perhaps indicating that electrons can hop between the Mn of different valences. This electron motion might contribute to a lowering of  $T_N$ .

A further possibility for the oxygen-annealed compound is that disorder caused by the oxygen reduces  $T_N$ . The diffraction pattern in Fig. 4(b) shows a large amount of diffuse scattering. This diffuse scattering arises from short-range correlations of magnetic defects, which could be partly or entirely responsible for the decrease in  $T_N$ . [There are also probably some macroscopic inhomogeneities in the oxygen content, as indicated by the small

shoulder above 100 K in the inset of Fig. 4(b); most of the temperature dependence, however, seems to be from a single order parameter.]

In conclusion, we have shown that the magnetic behavior of  $\text{BiPbCa}_2\text{MnO}_6$  is consistent with weakly ferromagnetic antiferromagnet, in which the spins are almost normal to the  $\text{MnO}_2$  planes in an antiferromagnetic arrangement, but are canted slightly toward the  $\text{MnO}_2$  planes. The canting direction is  $45^\circ$  to  $a$  or  $b$  along the Mn—O—Mn bonds. The isostructural compound  $\text{BiPbSr}_2\text{MnO}_6$  is similar in behavior for fields in the  $ab$  plane, suggesting a similar explanation, but its behavior for fields normal to the  $ab$  plane depends on the previous history, an aspect not yet understood.

#### ACKNOWLEDGMENTS

We are grateful to Rosi Hynes for orienting the crystal of  $\text{BiPbSr}_2\text{MnO}_6$ , and to Yvon Le Page for continuing advice on the structure of these materials.

<sup>1</sup>H. Maeda, Y. Tanaka, M. Fukutumi, and T. Asano, *Jpn. J. Appl. Phys.* **27**, L209 (1988).

<sup>2</sup>J. M. Tarascon, W. R. McKinnon, P. Barboux, D. M. Hwang, B. G. Bagley, L. H. Greene, G. W. Hull, Y. Le Page, N. Stoffel, and M. Giroud, *Phys. Rev. B* **38**, 8885 (1988).

<sup>3</sup>J. M. Tarascon, P. F. Miceli, D. M. Hwang, P. Barboux, G. W. Hull, M. Giroud, Y. Le Page, W. R. McKinnon, E. Tselepis, G. Pleizier, M. Eibschutz, D. A. Neumann, and J. J. Rhyne, *Phys. Rev. B* **39**, 11 587 (1989).

<sup>4</sup>Y. Le Page, W. R. McKinnon, J. M. Tarascon, and P. Barboux, *Phys. Rev. B* **40**, 6810 (1989).

<sup>5</sup>S. A. Sunshine, T. Siegrist, L. F. Schneemeyer, D. W. Murphy, R. J. Cava, B. Batlogg, R. B. VanDover, R. M. Fleming, S. H. Glarum, S. Nakahara, R. Farrow, J. J. Krajewski, S. M. Zahurak, J. V. Waszczak, J. H. Marshall, P. Marsh, L. W. Rupp, and W. F. Peck, *Phys. Rev. B* **38**, 893 (1988).

<sup>6</sup>J. M. Tarascon, W. R. McKinnon, Y. Le Page, K. Remschnig,

R. Ramesh, R. Jones, G. Pleizier, and G. W. Hull, *Physica C* **172**, 13 (1990).

<sup>7</sup>W. R. McKinnon, E. Tselepis, Y. Le Page, S. P. McAlister, G. Pleizier, J. M. Tarascon, P. F. Miceli, R. Ramesh, G. W. Hull, J. V. Waszczak, J. J. Rhyne, and D. A. Neumann, *Phys. Rev. B* **41**, 4489 (1990).

<sup>8</sup>J. M. Tarascon, Y. Le Page, W. R. McKinnon, R. Ramesh, M. Eibschutz, E. Tselepis, E. Wang, and G. W. Hull, *Physica C* **167**, 20 (1990).

<sup>9</sup>K. Remschnig, J. M. Tarascon, P. F. Miceli, G. W. Hull, and W. R. McKinnon, *Phys. Rev. B* **43**, 5481 (1991).

<sup>10</sup>D. E. Cox, G. Shirane, R. J. Birgeneau, and J. B. MacChesney, *Phys. Rev.* **188**, 930 (1969).

<sup>11</sup>J.-C. Bouloux, J. -L. Soubeyroux, G. Le Flem, and P. Hagenmuller, *J. Solid State Chem.* **38**, 34 (1981).

<sup>12</sup>T. Moriya, *Phys. Rev. B* **120**, 91 (1960).